Available online at www.sciencedirect.com
SCIENCE DIRECT
Talanta 69 (2006) 456–462
Talanta
www.elsevier.com/locate/talanta

Determination of 6-mercaptopurine based on the fluorescence enhancement of Au nanoparticles

Xing-Can Shen*, Ling-Feng Jiang, Hong Liang, Xin Lu, Lai-Jun Zhang, Xin-Yan Liu

College of Chemistry and Chemical Engineering, Guangxi Normal University, Guilin 541004, PR China

Received 15 March 2005; received in revised form 13 October 2005; accepted 13 October 2005
Available online 28 November 2005

Abstract

A novel method for the determination of 6-mercaptopurine (6MP) has been developed based on fluorescence enhancement of Au nanoparticles (AuNPs). The fluorescent AuNPs with mean diameter of ∼15 nm were synthesized in aqueous solution, exhibiting the stable maximum emission at 367 nm, under the excitation at wavelength of 264 nm. The AuNPs self-assembly with 6MP were characterized with transmission electron microscopy (TEM), ultraviolet–visible (UV–vis) absorption, fluorescence and surface-enhanced Raman scattering (SERS) spectroscopy. The results revealed that the surface attachment through versatile binding sites of S10, N3, N9 and N7 atoms in 6MP produced the interparticle coupling and formed aggregates of AuNPs. As a result, the fluorescence emission enhancement was significantly observed upon AuNPs self-assembly with 6MP. The fluorimetric determination under optimal conditions indicated that 6MP could be quantified in good linearity range of 6.35×10^{-8} to 3.05×10^{-7} M, with a low detection limit of 4.82×10^{-10} M. The relative standard deviation ($n = 11$) was 1.8% at 2.54×10^{-8} M 6MP concentration level. The proposed method was successfully applied for the determination of 6MP in spiked human urine. The probable fluorescence enhancement mechanism was also discussed there.

Keywords: Au nanoparticles; Fluorescence enhancement; 6-Mercaptopurine; Self-assembly; Interface interaction

1. Introduction

6-Mercaptopurine (6MP), a sulfur analogue of adenine (see Fig. 1) is one of the oldest anticancer drugs and immunosuppressive agents [1]. Since 1950s, 6MP has been applied to cure childhood and adult leukemias [2]. It has been established that 6MP and its metabolites exert their primary cytotoxicity through incorporation of deoxythioguanosine into DNA, and inhibit the function of RNaseH in DNA–RNA heteroduplex molecules [3]. Different analytical methods have been used for the determination of 6MP. It was found that the iodine–azide reaction of 6MP could yield a cathodic stripping signal at a sliver electrode, and the voltammetric response was used to detect 6MP over the range of 0.2–6 μM [4]. Removed protein from human blood plasma, 6MP and its metabolites could be detected in patient plasma by a reversed-phase high-performance liquid chromatography (HPLC) [5]. A DNA modified carbon paste electrode was applied for the determination of 6MP with a detection limit of 2.0×10^{-6} M [6]. However, most of these methods need sample pretreatments, or have relative low sensitivities. Therefore, it is necessary to develop a new direct, sensitive and facile assay method for 6MP.

Au nanoparticles (AuNPs) have attracted increasingly attention for the unique nano-optics properties. These fascinating optical properties, including those of surface plasmon band (SPB), surface-enhanced Raman scattering (SERS) and Raleigh resonance scattering (RRS), have been well documented [7]. These properties are very promising for DNA and RNA detection [8,9], immunoassay [10], medical diagnosis and sensors [11–13]. In contrast, the studies on photoluminescence from AuNPs are very limited [14–19]. For AuNPs or Au nanoclusters, emission lights in the near-IR [14], red [15] and blue [16–19] have been observed. Wilcoxon et al. reported the first observation of visible light emission from small AuNPs (∼5 nm) [16]. Zheng et al. synthesized blue emission eight-atom gold nanoclusters that encapsulated in dendrimers with a high quantum yield of ∼41% [17]. Using the fluorescence up-conversion technique and laser excitation, Kim et al. observed a weak

* Corresponding author. Tel.: +86 773 584 5495; fax: +86 773 584 5973.
E-mail address: xcshen@mailbox.gxnu.edu.cn (X.-C. Shen).

0039-9140/$ – see front matter © 2005 Elsevier B.V. All rights reserved.
doi:10.1016/j.talanta.2005.10.017

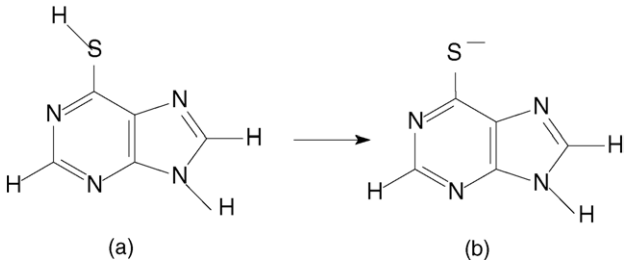

Fig. 1. (a) Thiol form of 6-mercaptopurine and (b) 6-mercaptopurine ion in aqueous solution.

femtosecond emission at 2.34 eV (530 nm) from the relatively large AuNPs (∼25 nm) [18]. Blue luminescence of Au nanoclusters embedded in silica matrix was reported recently [19]. Although photoluminescence phenomena of AuNPs have been observed, the potential applications of fluorescent AuNPs in biological and chemical assays are still scarce.

In the present work, the fluorescent AuNPs in aqueous solution were prepared with hydrothermal method. For AuNPs self-assembly with 6MP, the 367-nm fluorescence emission enhancement was proportional to the concentration of 6MP. Based on the experimental results, a novel direct and sensitive determination method for 6MP was developed. The interfacial interactions characters and probable fluorescence enhancement mechanism for AuNPs self-assembly with 6MP were also discussed there.

2. Experimental

2.1. Apparatus

The fluorescence spectra were recorded on an RF-5301 spectrofluorometer (Shimadzu, Japan) with 1 cm quartz cells. The light source used in the spectrofluorometer was a 150 W Xe arc lamp (Ushio Inc, Japan), and the emitted power density was approximately 20–32 mW cm^{-2} in its wavelength range. The slits for excitation and emission monochromators width were both 10 nm. The ultraviolet–visible (UV–vis) absorption spectra were recorded with a Cary-100 UV spectrophotometer (Varian, USA). Transmission electron microscopy (TEM) images of AuNPs were measured on an EM400ST transmission electron microscope (Philips, The Netherlands). The Raman and SERS spectra of 6MP were obtained with an inVia Raman Microscopes Spectrometer (Renishaw, UK), with a 514.5-nm argon ion laser performed as the excitation source. A DHG-101 cabinet-type thermostatically controlled furnace (Hualian, China) was served as heating source. A pHS-3B potentiometer (Leici, China) was used to measure pH values of solutions.

2.2. Reagents

6-Mercaptopurine monohydrate of 99% purity was purchased from Sigma Chemical Co., and used without further purification. Tetrachloroauric acid ($HAuCl_4$) and other chemicals were of analytical reagent grade and obtained from Shanghai Chemical Plant (China). The buffer of citric acid and sodium citrate solutions (0.01 M) was used to maintain pH. Stock solutions of 6MP (2.54×10^{-6} M, 1 l) were freshly prepared by dissolving the compounds in 2 ml NaOH solution (0.01 M), and then diluted with water. The doubly distilled, deionized water was used through the experiments.

2.3. Procedures

2.3.1. Preparation of AuNPs

The AuNPs were synthesized by the popular method of using citrate reduction of $HAuCl_4$ in aqueous solution [20]. Herein, the synthesis of AuNPs was improved using hydrothermal method. In a typical preparation, 5.0 ml $HAuCl_4$ solution (0.01%, m/v) was slowly added 4.0 ml sodium citrate solution (0.1%, m/v) with stirring, and diluted to 10.0 ml with water. The mixed solution was kept in an airtight reaction vessel, and heated with a thermostatically controlled furnace at 110 °C. The stable red gold colloid was obtained after heated for 1 h and allowed to cool to room temperature. The prepared gold colloid was adjusted volume (concentration of AuNPs: 2.9×10^{-2} mg ml^{-1}), and stored in glass containers at 4 °C. A series of gold colloids was prepared with the different dose of $HAuCl_4$ precursor (1.0–5.0 ml, 0.01%, m/v) and the same dose of sodium citrate (4.0 ml, 0.1%, m/v). For the prepared gold colloids, typical TEM images show that the diameters of the spherical AuNPs are about 15 nm, and the size distribution is homogeneous (Fig. 2A). The stability of the

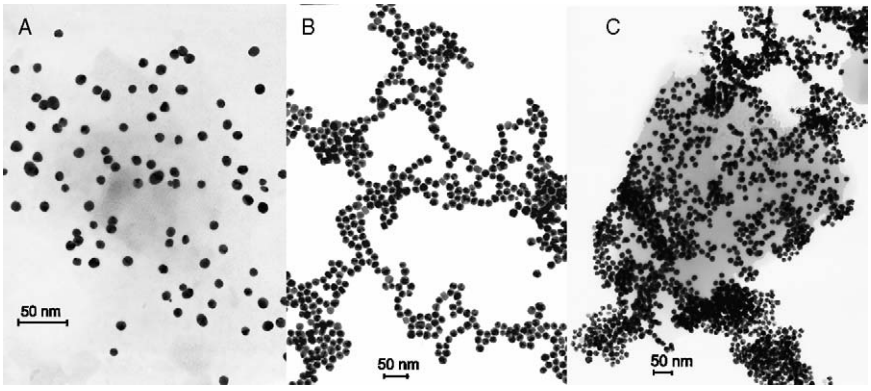

Fig. 2. TEM images of bare AuNPs (A) and AuNPs self-assembly with 6MP (B and C). Concentration of AuNPs: 5.8×10^{-3} mg ml^{-1}. Concentration of 6MP: (B) 1.27×10^{-8} M and (C) 3.81×10^{-7} M.

prepared gold colloids can be evaluated by monitoring absorption spectrum of AuNPs as a function of time [7,21]. Insignificant changes were observed for over 3 months, indicating that the prepared AuNPs had well stability in aqueous solutions.

2.3.2. AuNPs self-assembly with 6MP

The AuNPs self-assembly with 6MP were designed by introducing 6MP stock solutions into the prepared AuNPs at fixing concentration of 5.8×10^{-3} mg ml^{-1}. To a 10-ml volumetric flask, the reagents were added in the following order: 2.0 ml of the prepared gold colloid, 5 ml citrate buffer solution (0.01 M) and an appropriate volume of the 6MP stock solution (2.54×10^{-6} M). The mixture was diluted to 10.0 ml and stirred thoroughly. The AuNPs reacted with 6MP for ~3 h until the self-assembly equilibrium was reached.

2.3.3. Measurement of fluorescence spectra

The fluorescence spectra were obtained by scanning emission or excitation spectrum in the wavelength region from 200 to 700 nm on the spectrofluorimeter at the fixed excitation and emission wavelengths, respectively. The self-assembled AuNPs were used to assay 6MP directly via the changes of relative fluorescence emission intensities of the system. The enhancement of the emission intensity (ΔI) is the difference in intensities between the 6MP-modified AuNPs (I) and the bare AuNPs (I_0) in colloids.

2.3.4. Raman and SERS spectra measurements

The 6MP solution (10^{-3} M) was freshly prepared by dissolving the solid in slightly basic water (pH 7.43), to acquire the normal Raman spectrum. The prepared AuNPs colloid was used as the SERS-active substrate for detection the adsorbed 6MP. The sample for the SERS spectrum was a mixture of the 6MP solution and the prepared gold colloid, which was incubated for 3 h before the measurement. The final concentration of 6MP in gold colloid was about 10^{-5} M. The laser power at the samples was approximately 10 mW, and each spectrum was obtained in 30-s collection time.

3. Results and discussion

3.1. The characterizations of fluorescent AuNPs

As shown in Fig. 3a, the prepared 15-nm AuNPs exhibit a strong plasmon absorption band around 521 nm. The 521-nm SPB originates from the collective 6s electrons oscillations coupled through the surface to the electromagnetic field of the incoming light [7], which is the typical characteristic of AuNPs with the diameter larger than 2 nm [7,17]. The other outstanding feature in Fig. 3a is the appearance of a new shoulder band at 250 nm in the ultraviolet region. For fluorescent gold nanoclusters (4.2 nm), a similar absorption band at 270 nm appears in the ultraviolet region [16]. The probable fluorescence effect for the prepared 15-nm AuNPs was studied there. With the light excitation from a 150 W Xe-lamp, the strong light emission band at 367 nm (3.38 eV) was significantly observed with the 15-nm

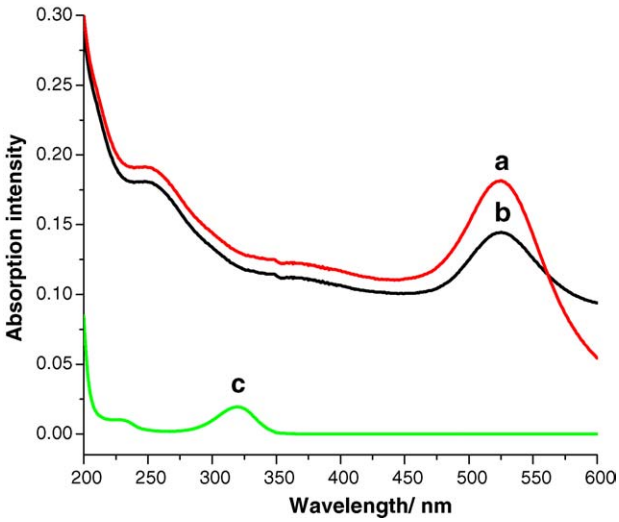

Fig. 3. UV–vis absorption spectra of AuNPs (a), AuNPs self-assembly with 6MP (b) and 6MP solutions (c). Concentration of AuNPs: 5.8×10^{-3} mg ml^{-1}. Concentration of 6MP: 1.27×10^{-8} M. Measurements performed in 0.01 M citric acid and sodium citrate buffer, pH 7.43.

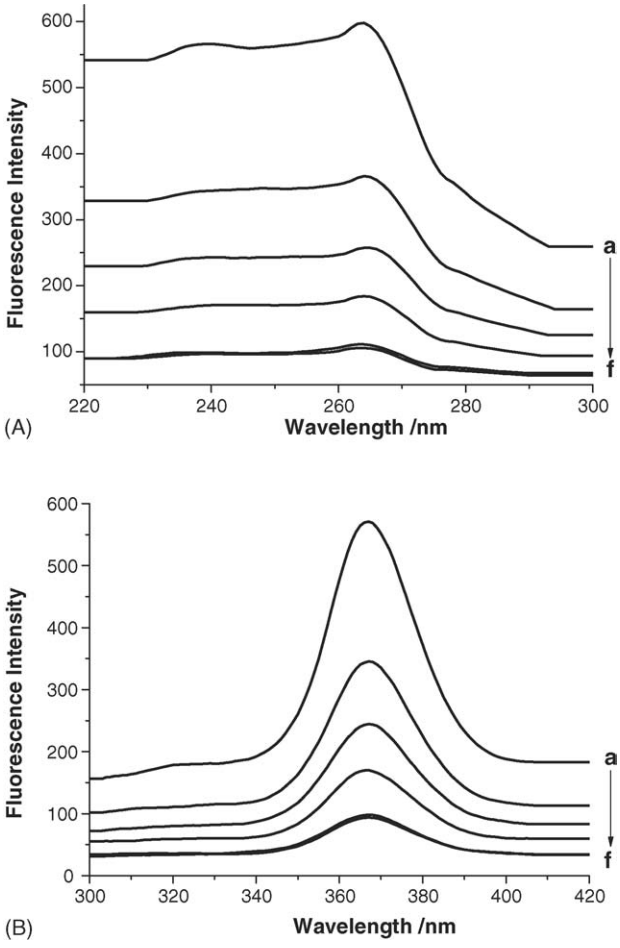

Fig. 4. (A) Fluorescence excitation spectra of AuNPs (λ_{em} = 367 nm) and (B) fluorescence emission spectra of AuNPs (λ_{ex} = 264 nm). AuNPs concentrations ($\times 10^{-3}$ mg ml^{-1}): (a) 29.0, (b) 23.2, (c) 17.4, (d) 11.6, (e) 5.8 and (f) 5.8. Measurement conditions: (a–e) performed in 0.01 M citric acid and sodium citrate buffer, pH 7.43 and (f) performed in 0.1 M citric acid and sodium citrate buffer, pH 7.43.

AuNPs in aqueous solution (Fig. 4B). The fluorescence excitation maximum at 264 nm (4.70 eV) was obtained by setting the emission detector to the 367 nm emission maximum (Fig. 4A).

A series of gold colloids containing 15-nm AuNPs of different concentration was prepared with the different dose of $HAuCl_4$ precursor and the same dose of sodium citrate. As shown in Fig. 4(a–e), the fluorescence excitation and emission intensities of these differently prepared gold colloids are directly proportional to the relative abundance of AuNPs, and no wavelength shift of the excitation and emission bands occurs. In these cases, the 15-nm AuNPs were prepared in water by sodium citrate reduction. The citrate ionic chemical has no detectable fluorescence. So, it is hard to accept the possibility that citrate ion is essential for the observed light emission. Wilcoxon et al. observed the visible light emission from the gold nanoclusters (~5 nm) reduced by citrate in water, as well as from the gold nanoclusters synthesized by the inverse micelle method [16]. There, it was found that the AuNPs added excess 10-fold dose of citrate ions yield indistinguishable fluorescence characteristics (Fig. 4(e and f)), suggesting the citrate ion has insignificant influence on the efficient emission from the 15-nm AuNPs.

The photoluminescence phenomena and relative mechanism of bulk Au and AuNPs have been investigated. At the excitation energy of 4.67 eV, fluorescence emission from smooth and rough Au films with the extremely low quantum efficiency of 10^{-10} was observed [22]. The gold nanoclusters (~5 nm) exhibited the visible emission at 440 nm (2.82 eV) [16]. The gold nanoclusters (<10 nm) embedded in SiO_2 matrix [19] and the water-soluble Au_8 nanodots showed blue luminescence [17]. Previous reports of the fluorescence emission from bulk Au [22] as well as from AuNPs [16,17,19] assigned the photoluminescence to an excitation of electrons from occupied d bands into states above Fermi level. Theoretical calculation indicated that interband transition from the d band to the Fermi level requires 2.4 eV of energy in gold [18,22]. There, at the excitation maximum of 264 nm (4.70 eV), strong fluorescence emission maximum at 367 nm (3.38 eV) was observed from the 15-nm AuNPs. Considering that the photoexcitation at 4.70 eV exceeds the interband energy, it is possible that electronic transition from d band to conduction sp-band above Fermi level occurs. Therefore, the probable fluorescence emission mechanism could be viewed as the recombination of conduction sp-electrons above Fermi level to occupied d-band holes, which is in agreement with the conclusions in previous reports [16,17,19].

3.2. The fluorescence enhancement of AuNPs self-assembly with 6MP

The absorption spectra of AuNPs before and after self-assembly are compared in Fig. 3(a and b), together with the spectrum of 6MP at the same conditions (Fig. 3c). As indicated in Fig. 3, the AuNPs self-assembly with 6MP are formed by judging from the spectral changes, including the absence of characteristic absorption bands of 6MP, the reduced absorption in the UV and visible range, a slight red-shifting and the obvious broadening of the 521-nm plasmon peak.

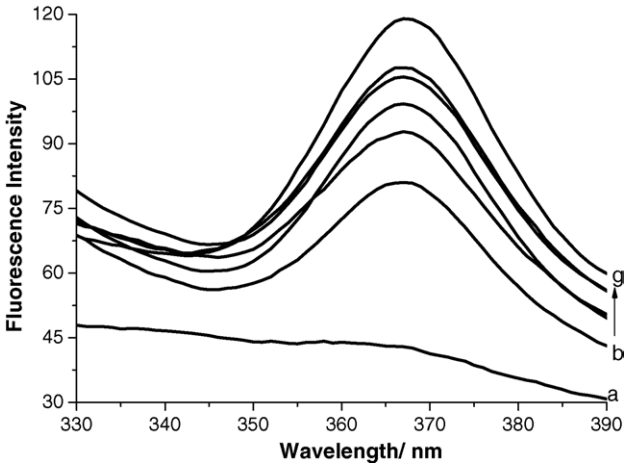

Fig. 5. Fluorescence emission spectra of 6MP (a) and AuNPs self-assembly with 6MP (b–g). 6MP concentrations ($\times 10^{-7}$ M): (a) 25.4, (b) 0, (c) 0.635, (d) 1.27, (e) 1.78, (f) 1.91 and (g) 3.05. AuNPs concentrations from (b) to (g): 5.8×10^{-3} mg ml^{-1}. Measurements performed in 0.01 M citric acid and sodium citrate buffer, pH 7.43.

Direct evidence concerning the morphology of self-assembled AuNPs comes from TEM images. As shown in Fig. 2B, the two-dimensional 6MP-linked AuNPs aggregates are formed, and the closely spaced clusters and strings are clearly present. The decreases of interparticle spacings and the formed linear aggregates with the elongated aspect ratios are also evident in Fig. 2B. It is well known that aggregation of AuNPs leads to a red-shifting and broadening of SPB [23]. Therefore, the TEM (Fig. 2B) results are consistent with the absorption spectral changes (Fig. 3).

The fluorescence emission spectra of AuNPs after self-assembly were obtained at different concentrations of 6MP, fixing the concentration of AuNPs. The fluorescence signal of free 6MP is weak, and no characteristic peak is observed in wavelength region of 340–390 nm (Fig. 5a). It is interesting to note that the fluorescence intensities of AuNPs are strongly enhanced after self-assembly with 6MP (Fig. 5(b–g)), and the enhancement of fluorescence intensity at 367 nm is proportional to the concentration of 6MP. The significant fluorescence enhancement of AuNPs and its potential applications in biological and chemical assays aroused our interest.

The photoluminescence properties of nanoparticles are strongly dependent on their size and shape [16–19,24,25]. Mohamed et al. reported a drastic increase (a million times) of the fluorescence from elongated AuNPs as compared to spherical particles [24]. The enhanced fluorescence emission associated with the formation of elongated nonspherical clusters was also present in the gold-dendrimer nanocomposites system [25]. It was reported that even for slightly elongated particles with the aspect ratios about 2, emission enhancement relative to the bulk metal may exceed a factor of 10,000 [24,25]. In this case, some linear aggregates of AuNPs with the elongated aspect ratios were produced after self-assembly with 6MP. Therefore, the enhanced fluorescence emission was suggestively due to local field enhancement caused by the elongated aggregates of self-assembled AuNPs.

3.3. The adsorption interactions of 6MP on the surface of AuNPs

The interface adsorption interactions of 6MP on the surface of AuNPs were investigated there. For the systems of AuNPs self-assembly with various sulfur containing ligands, it has been well established that aliphatic thiolate and aromatic dithiols are adsorbed on gold surface by forming one single Au–S covalent bond [26]. As being an aromatic thiol derivative, 6MP offers electronically and stereochemically versatile binding ability, and the possible binding sites to metals are N1, N3, N7 and N9, as well as the S10 atom attached to C6 of the purine ring [26,27]. However, the adsorption interaction of 6MP on the surface of AuNPs is still pendent. SERS spectroscopy provides a versatile approach for studying the interface interaction of adsorbed molecules [20,21,26–30]. It is well established that the aggregation of AuNPs is one of the widely used SERS-active substrates [20,21]. Therefore, the prepared AuNPs were used there as the SERS-active substrate to determinate the adsorption characteristic of 6MP on the surface.

Fig. 6(a and b) presents the Raman spectrum of solution 6MP and the SERS spectrum of 6MP adsorbed on AuNPs, respectively. As shown in Fig. 6a, the Raman spectrum exhibited typical vibration bands of solution 6MP, and the detailed assignment has been reported [27,28]. The calculated bands at 918.7 and 1407 cm^{-1} are assigned to S–H bending and N1–H deformation vibrations, respectively [27,28], which are absent from the Raman spectrum of solution 6MP (Fig. 6a). The result supports the view that the deprotonated 6MP anionic form (Fig. 1b) should exist in aqueous solution. Compared the spectrum Fig. 6(a and b), the outstanding feature is the appearance of the peaks at 217 cm^{-1}. Carron and Hurley assigned the 230-cm^{-1} band on the SERS spectrum of thiophenol to the Ag–S stretching [29]. The detected 217-cm^{-1} band in low-frequency region was assigned to Au–S stretching vibration there, which significantly revealed that 6MP adsorbed on the surface of AuNPs by forming Au–S covalent bond. Further evidence is provided with the obvious C6–S10 stretching vibration shifts: 420–398 and 1005–996 cm^{-1} (Fig. 6). The frequencies at 1290 and 1235 cm^{-1} in the solution spectrum of 6MP are the main contributions from C2–N3 stretching and N7–C8 stretching, respectively; the 1354- and 1430-cm^{-1} bands are assigned to C4–N9 stretching mode [27]. For these bands, the downshifts of −12, −10, −6 and −1 cm^{-1} are observed in SERS spectrum (Fig. 6b), respectively. The high enhancement at 697-cm^{-1} band assigned to the aromatic ring I vibration involving the N3–C4 stretching mode is detected in SERS spectrum (Fig. 6b). Moreover, the 572-, 865- and 950-cm^{-1} bands corresponding to ring I and ring II deformation modes are significantly enhanced in SERS spectrum (Fig. 6b). These results suggest that the surface attachment through N3, N9 and N7 atoms of 6MP with AuNPs is also likely. These findings are also substantiated by the calculations given by Szeghalmi, which reveal that N3, N9 and N7 atoms in 6MP have high negative partial charge that have a strong affinity for metal surface [26].

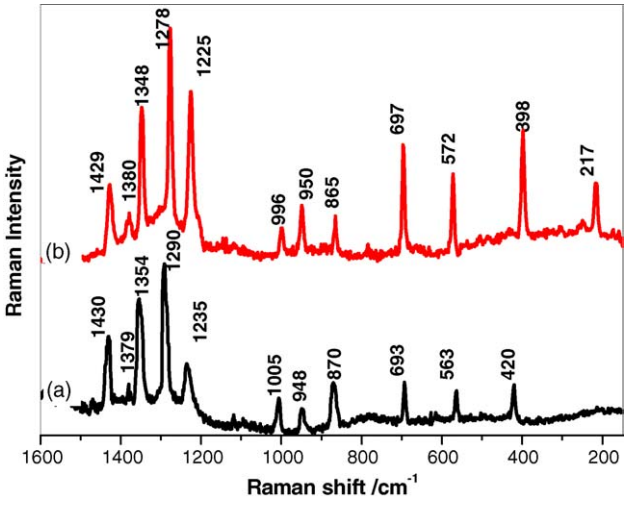

Fig. 6. (a) Raman spectrum of solution 6MP and (b) SERS spectrum of 6MP adsorbed on the surface of AuNPs.

Hence, the vibrational analysis of the SERS spectrum indicates that 6MP is covalently attached to AuNPs via the S10 atom. In addition, the adsorption interactions also probably occur through N3, N9 and N7 sites. It is inferred that the versatile binding sites of 6MP allow the molecule to be adsorbed by neighboring AuNPs, which produces the interparticle coupling and forms the aggregates of AuNPs. The aggregates of AuNPs observed in TEM images (Fig. 2B) are consistent with the conclusion.

3.4. Effect of pH and buffer solutions

The significant fluorescence enhancement allowed establishing a new approach for the determination of 6MP. The effects of selected experimental parameters on the assay method were investigated. It was found that the fluorescent AuNPs in aqueous solutions remained stable in the pH range of 5.0–9.0. The result is in agreement with the previous reported result [31]. Considering the AuNPs was prepared by citrate reduction, the buffer solution of citric acid and sodium citrate (0.01 M) was chosen to maintain the solution pH. The effect of solution pH on the fluorescence intensity of AuNPs was performed. The maximal fluorescent enhancement was observed when the pH values in the range of 6.45–7.73. The most suitable pH range of 6.45–7.73 is very close or identical to the pH of biological fluids, which helps to determinate 6MP directly in biological samples. There, the physiological pH 7.43 was chosen in the subsequent studies.

3.5. Effect of 6MP concentration

The suitable concentration range of 6MP for fluorescence enhancement was measured. It was found that fluorescence intensities increased as 6MP concentration increased from 0 to 3.05×10^{-7} M. The maximum fluorescence emission was attained when 6MP concentration was 3.05×10^{-7} M. Further increasing of 6MP concentration resulted in the precipitation of large aggregates of AuNPs, accompanied color changes of gold colloid from red to bluish-purple. As a result, the fluorescence intensities decrease and no longer concentration-dependent. The

TEM image (Fig. 2C) also shows that three-dimensional aggregates of 6MP-linked AuNPs at larger range are formed at higher concentration of 6MP. According, the concentration of 6MP should not be more than 3.05×10^{-7} M.

3.6. Effect of adding order

Studies on the adding orders showed that the efficient self-assembly of AuNPs depended on the adding orders of reagents. It was found that when the adding order was AuNPs, buffer and 6MP, both the stability and fluorescence signals were the best among the different mixing sequences. However, if the AuNPs and 6MP solutions were mixed firstly, fast precipitation of Au particles were often produced, which decreased the fluorescence intensities. Therefore, the adding order of AuNPs, buffer and 6MP solutions was adopted in the following studies.

3.7. Effect of self-assembly time

The effect of self-assembly time on the fluorescence intensity was investigated at room temperature. The fluorescence intensities at maximum emission wavelength of 367 nm were recorded at certain time intervals. As shown in Fig. 7, the fluorescence intensities increase with the increasing of self-assembly time until reaching the maximum of ~2 h, and then level off in the time range of 2–4 h. Further prolonging of accumulation time, however, results in the decrease of fluorescence intensity, suggesting too long reaction time might reduce the stability of self-assembled AuNPs. So, the accumulation time of 3 h was chosen for the following measurements.

3.8. Interferences of co-existing foreign substances

The interferences of co-existing foreign substances were tested under the above-selected conditions, spiked with different substances of a known concentration individually. An error of ±5% in the relative fluorescence intensity was considered tolerable. The results are summarized in Table 1. It can be seen from Table 1 that most of the tested substances including those of metal ions, some protein-forming amino acids, uracil, dextrose and glucosuria scarcely interfere with the determination

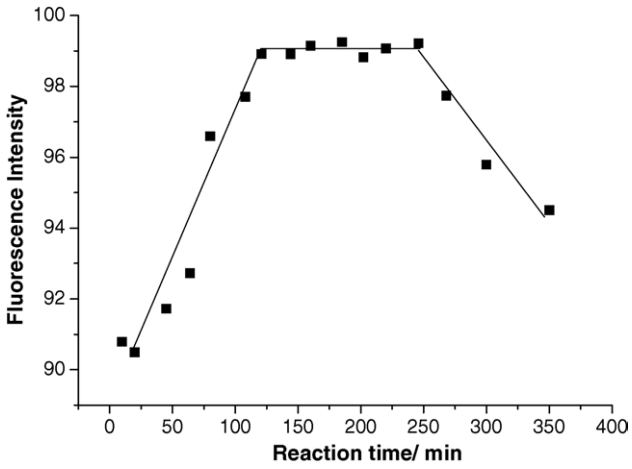

Fig. 7. Effect of reaction accumulation time on the fluorescence emission intensity at 367 nm. 6MP concentration: 1.27×10^{-8} M. AuNPs concentration: 5.8×10^{-3} mg ml^{-1}. Measurements performed in 0.01 M citric acid and sodium citrate buffer, pH 7.43.

at high tolerance levels. It is concluded that the method is free from many interferences of foreign substances. However, some substances such as adenine, cytosine, DL-cysteine and thiophenol could be tolerated only at relative low levels. It is noticeable that the tolerance level for cytosine is about 200-fold more than that of DL-cysteine. The facts indicate that interferences may be caused by the adsorption of these substances on the surface of AuNPs through functional groups such as thiols and amines, which influence the self-assembly of 6MP and change the fluorescence signal.

3.9. Analytical characteristics and applications

Using the optimized instrumental and operational parameters for 6MP standard solution, the linearity of the method was calculated and expressed. The regression equation was obtained by plotting ΔI (difference between fluorescence intensity of the 6MP-modified AuNPs and the bare AuNPs) versus 6MP concentration. The excellent linear range of the calibration graph was 6.35×10^{-8} to 3.05×10^{-7} M for 6MP. The fitted equation of this assay was $\Delta I = 4.843 + 1.096 \times 10^{8} C_{6MP}$ (M). The correlation coefficient was 0.9987, indicating a good linear correlation

Table 1
Interferences of co-existing foreign substances

Foreign substance	Concentration ($\times 10^{-5}$ M)	Change of FI[a] (%)	Foreign substance	Concentration ($\times 10^{-7}$ M)	Change of FI (%)
K^+, Cl^-	2.54	0.820	Aspartic acid	25.4	−2.36
Mg^{2+}, SO_4^{2-}	1.27	1.35	Tryptophan	12.7	3.08
Ca^{2+}, Cl^-	1.27	1.18	Tyrosine	12.7	3.08
Zn^{2+}, NO_3^-	0.508	−1.34	Lysine	2.54	4.85
Ni^{2+}, NO_3^-	0.508	2.31	Adenine	0.254	2.75
Glycine	1.27	2.65	Cytosine	0.254	2.75
Isolucine	0.508	4.45	DL-Cysteine	0.127	−3.39
Dextrose	0.508	4.45	Cystine	25.4	1.53
Uracil	0.127	3.08	Thiophenol	0.508	−4.19
Glucosuria	0.254	−2.36			

The concentration of 6MP was 2.54×10^{-7} M; measurements performed in 0.01 M citric acid and sodium citrate buffer, pH 7.43.
[a] FI: fluorescence intensity.

Table 2
Determination of 6MP in spiked human urine

Samples	6MP spiked ($\times 10^{-7}$ M)	6MP founded ($\times 10^{-7}$ M)[a]	Recovery (%)	R.S.D. (%)[b]
1	0.00	0.00	–	–
2	1.27	1.29	101.6	1.9
3	2.54	2.53	99.6	2.1
4	7.61	7.59	99.7	2.0

[a] Mean values of 11 determinations.
[b] Relative standard deviation.

between ΔI and the concentration of 6MP. The limit of detection was 4.82×10^{-10} M, and the relative standard deviation ($n = 11$) was 1.8% for determinations of 2.54×10^{-8} M 6MP in aqueous solution.

The proposed method was applied to the determination of 6MP in spiked human urine. The serum urine samples, obtained from healthy volunteers, were spiked with 6MP at different concentrations, and treated as the recommended procedure. The concentrations of 6MP were calculated from the calibration graph. The results obtained for the determination of 6MP in spiked human urine are given in Table 2. The satisfactory recoveries obtained with such a simple sample procedure are in the range of 99.6–101.6%. The proposed method provides higher sensitivity than that of previous methods [4–6], and the accuracy and precision of the results are also satisfactory.

4. Conclusion

The fluorescent AuNPs with mean diameter of ∼15 nm were synthesized in aqueous solution, exhibiting the stable fluorescent emission band at 367 nm, under the excitation at wavelength of 264 nm. The self-assembled of AuNPs with 6MP is obtained through forming covalent bonds adsorption with S10 and the surface attachment of versatile binding sites of N3, N9 and N7 atoms. As a result, the fluorescence emission intensities of AuNPs are significantly enhanced. Although understanding of the whole fluorescence enhancement mechanism was not complete in the present study, a novel and effective method for the determination of 6MP was developed based on the fact. The proposed method was satisfactorily applied for analysis of 6MP in human urine. The high sensitivity and simplicity of the assay method render it a very suitable method for determining 6MP at low levels.

Acknowledgements

The authors thank the financial support of National Natural Science Foundation of China (No. 20261001), Natural Science Foundation of Guangxi Zhuang Autonomous Region (No. 0339022), and Research Founding from the State Education Administration of China for Young Teacher.

References

[1] J.A. Montgomery, Prog. Med. Chem. 7 (1970) 69.
[2] L.W. Law, Proc. Soc. Exp. Biol. Med. 84 (1959) 409.
[3] J.A. Nelson, J.W. Carpenter, M.L. Rose, D.J. Adamson, Cancer Res. 35 (1975) 2872.
[4] B. Zeng, W.C. Purdy, Electroanalysis 10 (1998) 236.
[5] Y. Su, Y.Y. Hon, Y. Chu, M.E.C. Van de Poll, M.V. Relling, J. Chromatogr. B 732 (1999) 459.
[6] J.J. Zhu, K. Gu, J.Z. Xu, H.Y. Chen, Anal. Lett. 34 (2001) 329.
[7] M.-C. Daniel, D. Astruc, Chem. Rev. 104 (2004) 293.
[8] R. Elghanian, J.J. Storhoff, R.C. Mucic, R.L. Letsinger, C.A. Mirkin, Science 277 (1997) 1078.
[9] Y.C. Cao, R. Jin, C.A. Mirkin, Science 297 (2002) 1536.
[10] C. Zhang, Z. Zhang, B. Yu, J. Shi, X. Zhang, Anal. Chem. 74 (2002) 96.
[11] B. Dragnea, C. Chen, E.-S. Kwak, B. Stein, C.C. Kao, J. Am. Chem. Soc. 125 (2003) 6374.
[12] P. Pang, Z. Guo, Q. Cai, Talanta 65 (2005) 1343.
[13] S.D. Puckett, J.A. Heuser, J.D. Keith, W.U. Spendel, G.E. Pacey, Talanta 66 (2005) 1242.
[14] S. Link, A. Beeby, S. FitzGerald, M.A. El-Sayed, T.G. Schaaff, R.-L. Whetten, J. Phys. Chem. B 106 (2002) 3410.
[15] T. Huang, R.W. Murray, J. Phys. Chem. B 105 (2001) 12498.
[16] J.P. Wilcoxon, J.E. Martin, F. Parsapour, B. Wiedenman, D.F. Kelley, J. Chem. Phys. 108 (1998) 9137.
[17] J. Zheng, J.T. Petty, R.M. Dickson, J. Am. Chem. Soc. 125 (2003) 7780.
[18] Y.-N. Hwang, D.H. Jeong, H.J. Shin, D. Kim, S.C. Jeoung, S.H. Han, J.-S. Lee, G. Cho, J. Phys. Chem. B 106 (2002) 7581.
[19] S. Dhara, S. Chandra, P. Magudapathy, S. Kalavathi, B.K. Panigrahi, K.G.M. Nair, V.S. Sastry, C.W. Hsu, C.T. Wu, K.H. Chen, L.C. Chen, J. Chem. Phys. 121 (2004) 12595.
[20] P.C. Lee, D. Meisel, J. Phys. Chem. 86 (1982) 3391.
[21] K.C. Grabar, R.G. Freeman, M.B. Hommer, M.J. Natan, Anal. Chem. 67 (1995) 735.
[22] G.T. Boyd, Z.H. Yu, Y.R. Shen, Phys. Rev. B 33 (1986) 7923.
[23] A.A. Lazarides, G.C. Schatz, J. Phys. Chem. B 104 (2000) 460.
[24] M.B. Mohamed, V. Volkov, S. Link, M.A. El-Sayed, Chem. Phys. Lett. 317 (2000) 517.
[25] O. Varnavski, R.G. Ispasoiu, L. Balogh, D. Tomalia, T. Goodson III, J. Chem. Phys. 114 (2001) 1962.
[26] A.V. Szeghalmi, L. Leopold, S. Pînzaru, V. Chis, I. Silaghi-Dumitrescu, M. Schmitt, J. Popp, W. Kiefer, J. Mol. Struct. 735–736 (2005) 103.
[27] A. Vivoni, S.-P. Chen, D. Ejeh, C.M. Hosten, Langmuir 16 (2000) 3310.
[28] A. Vivoni, S.-P. Chen, D. Ejeh, C.M. Hosten, J. Raman Spectrosc. 32 (2001) 1.
[29] K. Carron, L.G. Hurley, J. Phys. Chem. 95 (1991) 9979.
[30] C.R. Yonzon, D.A. Stuart, X. Zhang, A.D. McFarland, C.L. Haynes, R.P. Van Duyne, Talanta 67 (2005) 438.
[31] G.B. Sergeev, Russ. Chem. Rev. 70 (2001) 809.